Deformation behavior and mechanical properties of hard elastic and porous films of polyethylene

Galina Elyashevich*, Evgenii Karpov, Alexandr Kozlov

Institute of Macromolecular Compounds, Russian Academy of Sciences
199004 St.Petersburg, Russia

SUMMARY: Hard elastic samples of linear polyethylene were prepared by melt extrusion at a high velocity of the melt flow and by subsequent annealing of crystallized samples. The deformation behavior of hard elastic samples obtained by annealing of as-spun samples at different temperatures has been analyzed at uniaxial extension resulting in formation of porous structure. Mechanical properties of microporous films in the longitudinal and transverse directions have been investigated. Composite systems consisting of a microporous polyethylene film and a thin layer of an electroconducting polymer have been prepared. Mechanical properties of composite systems, such as elastic modulus, tensile strength, and break elongation, have been compared with the properties of polyethylene substrates.

Introduction

In recent years, microporous polymer films have been widely used for practical purposes such as filtration and separation of liquid mixtures, and also as separation membranes in chemical batteries. The separator divides the anodic and cathodic spaces in a battery and prevents countercurrent and self-discharge. Properties of porous films used as separators should meet certain requirements, such as high permeability, chemical stability, and high mechanical characteristics.

We have developed a procedure for preparing microporous, highly permeable polyethylene (PE) films which are based on extrusion of PE melt[1)]. Chemical resistance to organic solvents, acids, and alkalis, which allows the use of PE films in batteries with both aqueous and nonaqueous electrolytes, and also high mechanical characteristics of these films make PE microporous films the most suitable separation material for chemical batteries.

Porous structure formation process

High-density linear PE with M_w 1.4 x 10^5, M_w/M_n 6-8 and melting temperature T_m 132 °C was used to prepare porous films. Formation of the porous sample structure proceeds in several stages (Fig. 1).

 CCC 1022-1360/99/$ 17.50+.50/0

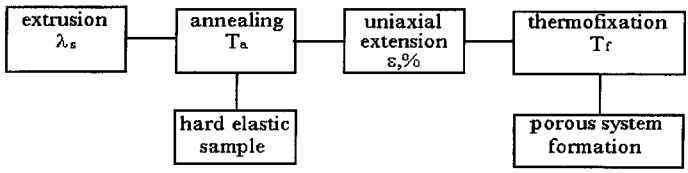

Fig. 1 Schematic representation of porous film formation process

The first stage - extrusion - is the stage of film formation when the melt is oriented at a high velocity of the flow and then crystallizes at room temperature. As a result, an oriented crystalline structure consisting of a system of large lamellar crystals in the form of thin planes arranged parallel to each other and perpendicular to the orientation direction and connected with a number of tie chains is formed (Fig. 2).

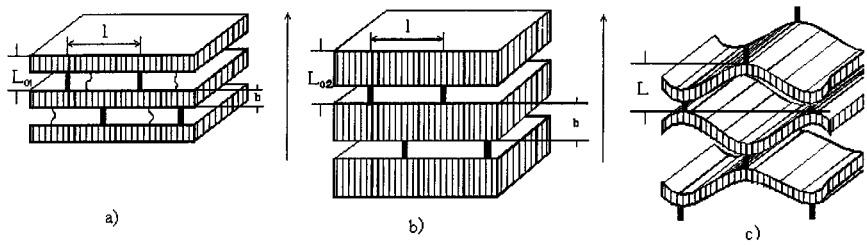

Fig. 2 Structure model of PE samples at different stages of the porous structure formation: a) as-spun; b) annealed (hard elastic); c) porous structure formation at uniaxial extension (the extension direction is shown by the arrow). L_{01} is the long period in the initial (as-spun) PE, L_{02} is the long period in the annealed PE, L is the long period after extension, b the lamellar thickness, l the distance between ties, d the transverse size of lamellae

The second stage - annealing at the temperatures close to T_m under the conditions preventing shrinkage of PE - leads to an increase in the orientation degree and thickness of lamellae due to involving molecular chains from amorphous regions in the crystals. As a result, the number of tie chains decreases, they become fully extended and connect the lamellae as stressed links (hard "bridges") which are statistically distributed over the lamellar surface (Fig. 2b). The mechanical properties of such highly oriented samples can be described as hard elastic because they are characterized not only by a rather high elastic modulus, but also by a high elastic recovery typical of elastomers [2-5].

These properties give a possibility to extend annealed films at the third stage of the process several times without breaking. No necking is observed at this extension. Uniaxial deformation of hard elastic samples in the orientation direction leads to moving apart and

bending of lamellae between tie points, and, as a consequence, to the appearance of discontinuities (pores) between them (Fig. 2c).

The fourth stage is the thermofixation of porous structure, i.e., keeping the sample with fixed size for a certain time at elevated temperatures for relaxation of the stress in the stretched sample. This treatment at the final stage of the porous structure formation excludes shrinkage of the sample after removal of deformation stress. Temperature at this stage of the process, T_f, controls the thermal stability of porous films which manifests itself when porous films show shrinkage in heating. The capability of shrinking is very important for the use of these films as a separation material for chemical batteries. For instance, lithium batteries should not be heated above 80 - 100 °C to prevent possible inflammation and even explosion of the battery. Utilization of PE separators excludes such processes because, at critical temperatures, this material shrinks, closing pores and terminating overheating.

Mechanical behavior of hard elastic samples at deformation

The mechanical properties and permeability of porous samples are controlled by numerous parameters at each stage of the process. Being a percolation phenomenon, permeability is determined by the appearance of through-flow channels[6,7] which are formed in the sample only under definite conditions of the porous structure formation process, namely, at definite values of thermal and orientational parameters - spin draw ratio, annealing temperature, and degree and rate of extension[1,7]. Hence, it is very important to clarify the effect of various parameters on structure and properties of hard elastic and porous samples.

Mechanical behavior of hard elastic systems at deformation can be demonstrated by the stress-strain curve (Fig. 3).

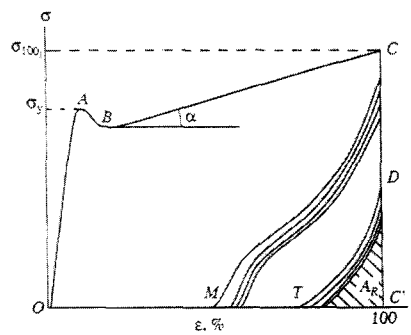

Fig. 3 Stress-strain curves at cyclic extension for hard elastic PE samples: σ_y yield stress point; σ_{100i} stress at maximal extension in this cycle, E_R elastic recovery (ratio MC'/OC'), A_R work recovery (dashed part of the curve CC'T), A_R/A_D the portion of work recovery in the full work at extension (ratio of areas CC'T/MCC' in the cycles following the first one and the ratio CC'T/OCC' in the first cycle).

The initial linear part of curve OA describes elastic deformation of the sample up to the yield stress σ_y. The elastic modulus in this part of the curve is determined only by amorphous regions in the sample where tie chains bear the main load.

In the second part of curve ABC (post-yield region), the profile of the curve dramatically changes: after a short intermediate process AB, a linear increase in the stress is observed, but the slope of this straight line becomes significantly smaller. The measurements of the restoring force have led Park and Noether[3] to the conclusion that the elasticity has the energetic origin in this case; they related this kind of elasticity to the lamellar bending in the deformation process. The elastic character of the lamellar bending is responsible for a stress increase in the second stage of deformation.

If the second part of the stress-strain curve is associated only with the purely elastic deformation of lamellar bending, the slope of this part of the curve should depend only on the elastic modulus of the lamellar network. However, extension of a real lamellar network with a random distribution of stretched tie chains gives rise not only to the elastic lamellar bending, but also to some irreversible processes that change the slope of the stress-strain curve. These irreversible processes involve the breakdown of some tie chains and of the weakest links as well as pulling of some tie-chains through crystallites[8] and splitting of crystallites. As a result, displacement of some network fragments with respect to each other takes place, and the entire lamellar network experiences dramatic structural changes.

These processes, together with the relaxation processes in amorphous regions, contribute to the value of stress at this stage of extension of hard elastic samples and control the slope of the BC region of the curve in Fig. 3. As it was proved by our experiments, the slope of this part of the curve depends on the spin draw ratio λ_s, i.e., on the orientation degree which was reached at the first stage of the structure formation process. This means that the orientation degree affects the deformation characteristics of a hard elastic system in this part of the curve.

Hence, at the second stage of extension, two deformation modes are involved: elastic recovery of lamellar network and irreversible deformation accompanied by changes of the lamellar network as a whole. On passing from the first part of the extension curve to the second, the uniform elastic deformation mode changes to another deformation mode which involves both elastic and plastic components. This transition is preceded by a certain decrease in stress which is observed when the yield point is attained (part AB in Fig. 3).

Once the extension is stopped (point C, Fig. 3), irreversible processes, which can be regarded as viscous flow, cease and their contribution to the deformation stress vanishes. The stress

almost immediately drops to the stress corresponding to elasticity of the lamellar network (point D in Fig. 3).

During the recovery process, when the distance between the fixed ends of the test sample decreases at a constant strain recovery rate, the stored elastic energy of lamellar bending is released, and the stress still goes down. For an ideal lamellar network, this process should be described by a linear dependence passing through the points D and M, where the position of point M characterizes the fraction of elastic recovery in the total value of deformation. However, the macromolecular chains with extended conformations (as a result of extension) between the regions of lamellae which have moved apart hinder fast recovery of the initial form of lamellae because any conformational change is a relaxation process and requires a certain time. The process of strain recovery is characterized by a certain rate, and the stress-strain curve is therefore located below the straight line DM and intersects the abscissa axis in point T. The value of elastic recovery E_R which is equal to the MC' fragment appears to be rather high and reaches 60 % of the total tensile strain.

The behavior of hard elastic samples at deformation was studied also at cyclic loading. The loading - unloading cycles are characterized by similar deformation patterns, except for a slight shift of the curve to larger strains: each subsequent curve lies somewhat below the curve for the preceding cycle. This behavior is related to the continuous disruption of the stressed links between lamellae. Since this disruption is the thermofluctuational process[9], some of these links that have survived during the first cycle break down during the following loading - unloading cycles. The elastic modulus of the lamellar network decreases, and the stress appears to be lower at the same tensile strain. In repeated loading - unloading cycles, the number of weak links decreases, the number of disruption events also decreases and, after each cycle, the stress-strain curves move closer and closer to each other and finally almost coincide.

The effect of annealing temperature on the mechanical behavior of hard elastic samples

As it was observed in Ref.[10], the permeability of porous films obtained by extension of hard elastic samples is strongly dependent on T_{ann}, the annealing temperature of as-spun films. Moreover, permeable porous films are formed only if the annealing temperatures are higher than 100 °C and permeability sharply increases when T_{ann} approaches the melting temperature T_m. This means that T_{ann} is the percolation parameter and has a threshold value equal to 100 °C, i.e., through-flow channels appear in porous samples only when T_{ann} lies in a rather narrow temperature interval between the threshold temperature and T_m.

We studied the effect of annealing temperature on the basic parameters of the stress-strain curve. It was found that the dependences of all these parameters - yield stress, slope angle α, σ_{max}, elastic recovery and work recovery (Fig. 3) - on T_{ann} are characterized by well pronounced maxima, but these maxima are associated with three different annealing temperatures. With respect to their positions on the temperature axis, these maxima can be conditionally divided into three groups corresponding to three parts of the stress-strain curve.

The dependence of the yield stress on T_{ann} shows a very narrow maximum at the highest temperature 130 °C close to the melting temperature (Fig. 4a). It should be noted that the profile of this dependence is absolutely similar to the profiles of the dependences of the X-ray long period (see Fig. 2) and permeability on T_{ann}[1,10]. The maxima of dependences of angular coefficient tan α and stress at maximal strain σ_{max} on T_{ann} are observed at 125 °C (Fig. 4b). Finally, the dependences of elastic recovery E_R and work recovery A_R/A_D on annealing temperature show maxima at T_{ann} = 115 °C (Fig. 4c).

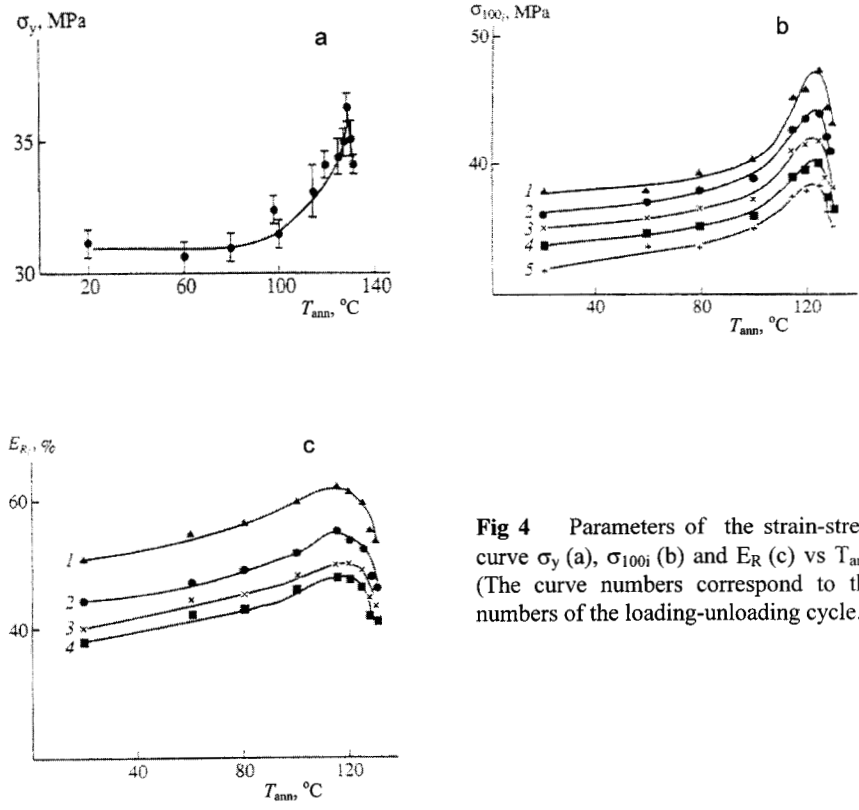

Fig 4 Parameters of the strain-stress curve σ_y (a), σ_{100i} (b) and E_R (c) vs T_{ann}. (The curve numbers correspond to the numbers of the loading-unloading cycle.)

The nature of these maxima and their positions along the temperature axis can be interpreted within the framework of the structure model of Fig. 2. It is well known[11] that the X-ray period, L_0, and also the fold size, b, sharply increase when T_{ann} approaches the melting temperature of crystals. At T_{ann} below 80 °C, these structure parameters do not change because at low annealing temperatures, there are no considerable structural transformations, and only perfection of the crystalline structure owing to elimination of various defects and "smoothing" of the folded surface of lamellae may occur.

At T_{ann} > 80 °C, the fold size starts to increase because of involving tie chains in crystals. This process leads to a decrease in the lengths of tie chains which approach the thickness of the amorphous regions; their length distribution becomes narrower and the number of stressed tie chains increases. As a result, the initial elastic modulus and the number of tie chains which simultaneously break at the yield point increase thereby providing an increase in σ_y with T_{ann}. The increase in the number of broken tie chains leads in turn to a decrease in the number of links between lamellae, and hence to an increase in the pore size and their total volume, including the appearance of through-flow channels responsible for permeability of samples.

This conclusion is confirmed by the fact that the samples annealed at temperatures above 100 °C are permeable to liquids, the permeability increasing with T_{ann} up to the melting temperature. This consideration explains the similar profiles of dependences of σ_y and the X-ray long period of annealed samples, and permeability of porous films on T_{ann}. The decrease in these parameters when T_{ann} is nearly equal or higher than T_m of nonstressed samples is associated with partial melting of initial crystallites and subsequent recrystallization at lower temperatures.

It can be seen in Fig. 4b that as T_{ann} grows, the slope of the second part of the stress-strain curve becomes steeper due to an increase in the elastic modulus of lamellar network associated with lamellar bending. As the annealing temperature approaches T_m, the length distribution of tie chains becomes very narrow because almost all chains are extended and equally stressed, and they break down simultaneously. In this case, the number of links between lamellae decreases so fast that a drop in the elastic modulus of lamellar network is observed. This manifests itself in a decrease in angle α when the annealing temperature approaches T_m. As a result, the maxima of the tan $\alpha(T_{ann})$ and $\sigma_{max}(T_{ann})$ dependences are located at temperatures below T_m, near 125 °C.

The transformation of lamellar network which leads to an increase in its elastic modulus with T_{ann} is responsible for an increase in the values of elastic recovery and work recovery (Fig. 4c). However, the breakdown of links between lamellae, which changes lamellar network

itself, makes an additional contribution to the irreversible component of strain in the second part of the curve and also reduces the stored elastic energy of the stressed lamellar network. Finally, the work recovery in the third part of the curve decreases. The intensity of these processes dramatically increases when the annealing temperature approaches T_m. As a result, both E_R and A_R/A_D decrease and the onset of this decrease is observed at lower temperatures (115 °C) (Fig. 4c) as compared with the decrease in the characteristics describing the second part of the curve (Fig. 4b).

The investigations of the structure and mechanical behavior of hard elastic PE films have demonstrated that the structure parameters, such as the long period and permeability and also the yield stress, increase monotonically with T_{ann} up to the melting temperature of crystals. At the same time, the parameters associated with elastic properties of hard elastic PE pass through maxima at T_{ann} = 125 °C lower than T_m. The dependences of the parameters related to elastic recovery on T_{ann} show maxima at even lower T_{ann} = 115 °C. The above evidences allow to conclude that the elastic properties of hard elastic materials are controlled not only by the thickness of lamellae, but also by the length distribution of tie chains, which demonstrates dramatic changes depending on annealing temperature.

It should be noted that the result of the deformation process of hard elastic PE strongly depends on the rate of extension[1,7]. At low extension rates, the pore formation process is dominated by the orientational strengthening which leads to transformation of the initial lamellar structure into the fibrillar structure resulting from turning lamellae and unfolding chains. It is well known[12] that orientational strengthening proceeds most successfully at low rates of deformation. At high deformation rates, the destruction of structure competes with the pore formation because in the drastic regime of deformation, splitting of crystals and fracture of lamellae themselves take place. Both orientational strengthening and disruption hinder the pore formation; however, there is an interval of rates where pore formation turns out to be prevailing. This fact is evidenced by a strong maximum in the dependence of permeability on the deformation rate and by the existence of intervals of deformation rates on both sides of the permeability maximum where through-flow channels are not formed and permeability is not observed.

Mechanical properties of porous films and composite membranes

Consideration of mechanical behavior of hard elastic PE at deformation is especially important because their ability to reversibly deform gives a possibility to realize the transformation of these samples into a porous system by uniaxial extension. Of major interest

are observations of the porous structure formation which demonstrate the reversible character of deformation of hard elastic samples directly in the X-ray camera[14]. Formation of micropores was accompanied by a sharp increase in the integral scattering intensity so that for an 80 % deformation, a thirteen-fold increase in the intensity was observed. The dependence of intensity on deformation is reversible, i.e., as deformation decreases, the intensity values repeat in the reverse order. If we regard the porous film as a two-phase system, where the first phase is PE and the second phase is cavities, the increase in the integral scattering intensity from a porous sample by an order of magnitude compared with that from an annealed film and its growth with extension of a hard elastic sample indicate that the volume fraction of the second phase becomes larger when the extension degree increases. This result is confirmed by the data showing that the permeability of porous films becomes higher due to an increase in the number of flow-through channels with increasing extension degree at the stage of pore formation[7].

However, both the X-ray and optical scattering are produced not only by pores in the sample bulk. It was observed in electron microscopic[6] and optical investigations[13,14] that porous films are characterized by a pronounced relief-like surface which also makes a contribution to the scattering pattern. As it was found in Refs.[15,16], electroconducting polymer layers produced by polymerization in the gas phase (polyacetylene, polypyrrole) or by deposition of dispersion (polyaniline, polypyrrole) show a very high adhesion to the surface of porous PE films. Since the conventional PE films obtained by melt extrusion as well as our as-spun and annealed films have no adhesion to any polymeric and nonpolymeric coatings, it is possible to conclude that a high adhesion of our porous films is provided by a specific relief-like character of their surfaces. The suggestion that there is no interaction between the PE film and a deposited layer of conducting polymer is confirmed by IR investigations[17].

High mechanical properties - high strength and elasticity - together with a good adhesion to different coatings make our porous PE films suitable elastic substrates for advanced materials such as electroconducting polymers. These polymers have very poor mechanical properties - low strength and high brittleness; moreover, some of them are not capable of film formation. Additionally, it appeared that the layer of a conducting polymer (polypyrrole) on the polyimide substrate provides such a high brittleness to the whole system that it becomes fully deformed and unusable. In contrast, the composite membranes consisting of our porous PE film with a thin conducting polymer layer demonstrate high mechanical properties. We have investigated mechanical properties of composite membranes with layers of polyacetylene, polyaniline and polypyrrole[15,16,18]. The most surprising feature of mechanical properties of

these composites is a combination of the increased elastic modulus and break elongation of composites compared with the corresponding values of porous PE films (see Table 1).

Table 1 Mechanical properties of porous films and composites

Composite	Tensile strength σ MPa	Elastic modulus E MPa	Breaking elongation ε %
PE	100	1000	30
PE - polyacetylene	132	1300	36
PE - polyaniline	143	1800	40
PE - polypyrrole	155	2200	50

The increase in the elastic modulus is easily explained by depositing the layer of rigid-chain conducting polymer on the oriented PE film, while the increase in the break elongation may be explained by a possible plastification effect. No decrease in the strength of porous PE films after deposition of conducting polymer layers was observed. High mechanical properties make porous PE films and composites based on them very attractive for the use as membrane-separation elements in chemical batteries and as ion-exchange membranes in electrochemical processes.

Acknowledgment
This work was supported by Russian Foundation for Basic Research (Grant No. 98-03-33384a).

References

[1] G.K. Elyashevich, A.E. Bitsky, A.G. Kozlov, E.Yu. Rosova, *Russ. J. Appl. Chem.* **70,** 1114 (1997)
[2] B.S. Sprague, *J. Macromol. Sci.* **8,** 157 (1973)
[3] I.K. Park, H.D. Noether, *Colloid Polym. Sci.* **53**, 824 (1975)
[4] S.I. Cannon, G.B. McKenne, W.O. Statton, *J. Macromol. Sci., Macromol. Rev.* **11**, 209 (1976)
[5] G.K. Elyashevich, E.Yu. Rosova, E.A. Karpov, *Vysokomol. Soedin. B* **33**, 723 (1991)
[6] O.V. Kudasheva, E.Yu. Rosova, E.A. Karpov, G.K. Elyashevich, *Polym. Sci. A (translated from Russian)* **39**, 1095 (1997)
[7]) G.K. Elyashevich, A.G. Kozlov, E.Yu. Rosova, *Polym.Sci. A (translated from Russian)* **40**, 567 (1998)
[8] I.M. Ward, M.A. Wilding, *J. Polym. Sci., Polym. Phys. Ed.* **22**, 961 (1984)
[9] V.R. Regel, A.I. Slutsker, E.E. Tomashevskii, *Kineticheskaya Priroda Prochnosti Tverdykh Tel (Kinetic Nature of the Strength of Solids),* Nauka, Moscow 1974, p. 238
[10] E.A. Karpov, V.K. Lavrentev, E.Yu. Rosova, G.K. Elyashevich, *Polym. Sci A (translated from Russian)* **37**, 1247 (1995)
[11] B. Wunderlich, *Macromolecular Physics*, Vol 2, Academic Press, New York 1976
[12] V.A. Marikhin, L.P. Myasnikova, *Nadmolekulyarnaya Struktura Polimerov (Supermolecular Structure of Polymers)*, p. 67, Khimiya, Leningrad 1977
[13] G.K. Elyashevich, A.G. Kozlov, A.P. Kovshik, E.I. Ryumtsev, *Opt. Zh. (Russian),* **65**(7),

51 (1998)
[14] G.K. Elyashevich, A.G. Kozlov, I.T. Moneva, A.A. Zinchik, A.V. Smirnov, S.K. Stafeev, *Proceedings of Int. Soc. Opt. Eng. (SPIE),* v. 3573, p. 296-299, 5th Congress of Modern Optics OPTIK'98, Budapest 1998
[15] G.K. Elyashevich, A.G. Kozlov, N. Gospodinova, P. Mokreva, L. Terlemezyan, *J. Appl. Polym. Sci.* **64**, 2665 (1997)
[16] E.Yu. Rosova, G.A. Polotskaya, A.G. Kozlov, G.K. Elyashevich, M. Bleha, V. Kudela, *Polym. Sci. A (translated from Russian)* **40**, 530 (1998)
[17] G.K. Elyashevich, A.G. Kozlov, E.Yu. Rosova, M. Bleha, *Preprints Int. Conf. Membr. Sci. Technol. (ICMST '98)*, p. 67, Beijing, China, June 9-13, 1998
[18] D.G. Belov, T.N. Danilchuk, O.N. Efimov, G.K. Elyashevich, A.T. Ponomarenko, I.N. Chmutin, *Abstracts 4th Int. Symp. Polymers for Advanced Technologies, PAT-97,* Leipzig, Germany, P II.2 (Aug. 31 - Sept. 4, 1997)